Supplementary Information

High-Throughput Bacterial Co-Encapsulation in Microfluidic Gel Beads for Discovery of Antibiotic-Producing Strains

Abraham Ochoa,[a] *Gabriela Gastélum,*[b] *Jorge Rocha* [c] *and Luis F. Olguin* *[a]

[a] Laboratorio de Biofisicoquímica, Facultad de Química, Universidad Nacional Autónoma de México, *Coyoacán, CDMX 04510, México.*
E-mail: olguin.lf@quimica.unam.mx

[b] Unidad Regional Hidalgo, Centro de Investigación en Alimentación y Desarrollo A.C., *San Agustín Tlaxiaca, Hidalgo 42163, México.*

[c] Programa de Agricultura en Zonas Áridas, Centro de Investigaciones Biológicas del Noroeste. *La Paz, B.C.S. 23096, México.*

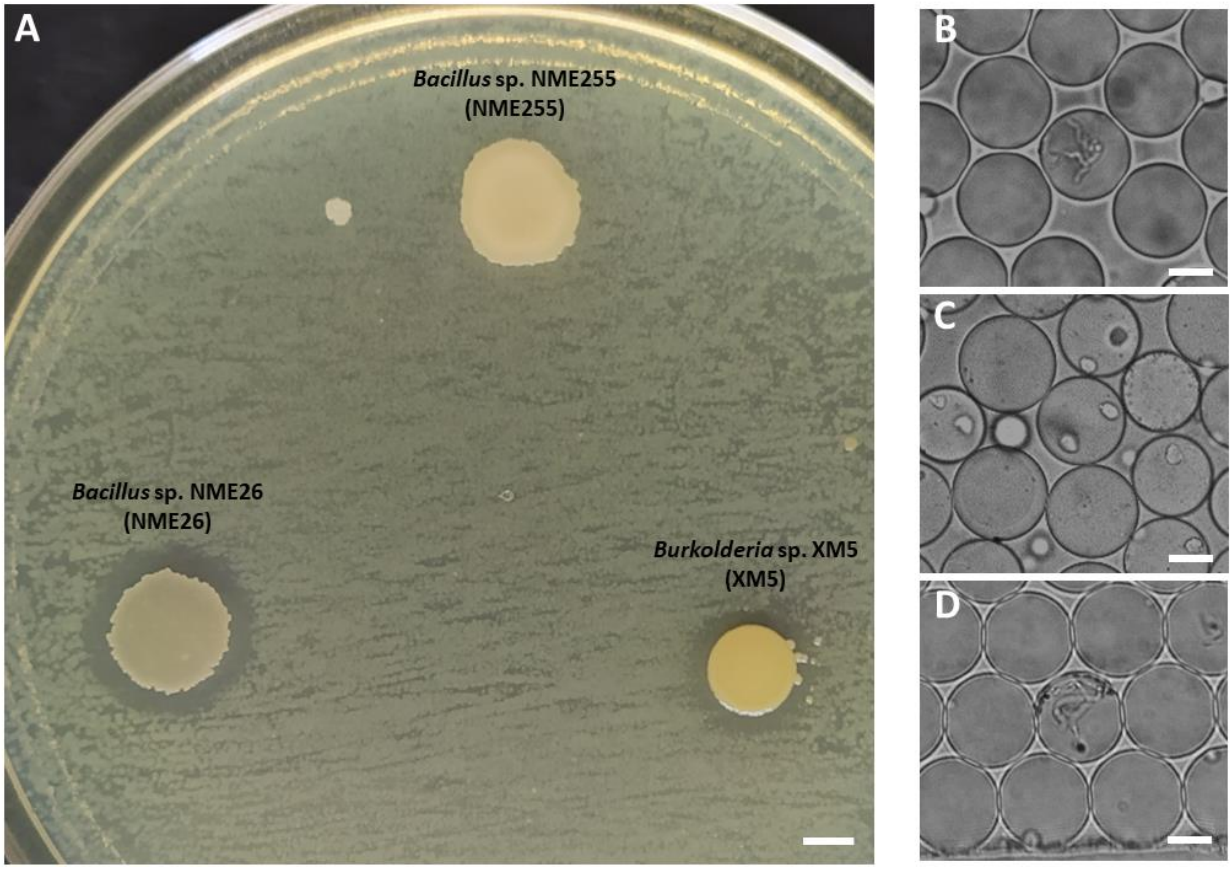

Figure S1. (A) Spot-on-lawn assay for growth inhibition of *E. coli* by three different bacteria isolated from the rhizosphere of Mexican maize. The entire agar surface was inoculated with *E. coli-GFP*. Then, using frozen stocks, the same surface was spot inoculated with each maize bacteria strain. After 48 h incubation at 27 °C, all strains grew. Each strain is easily distinguishable according to colony morphology. NME255 did not show inhibition activity, XM5 has a moderated antagonistic activity and NME26 presented the strongest antagonistic activity against *E. coli-GFP* growth, Scale bar 0.5 cm. (B-D) The three strains from maize were independently encapsulated into gel beads. After 18 h of incubation bacterial growth for each strain into beads was analyzed by bright-field microscopy: (B) NME255; (C) XM5; (D) NME26, scale bar 10 µm.

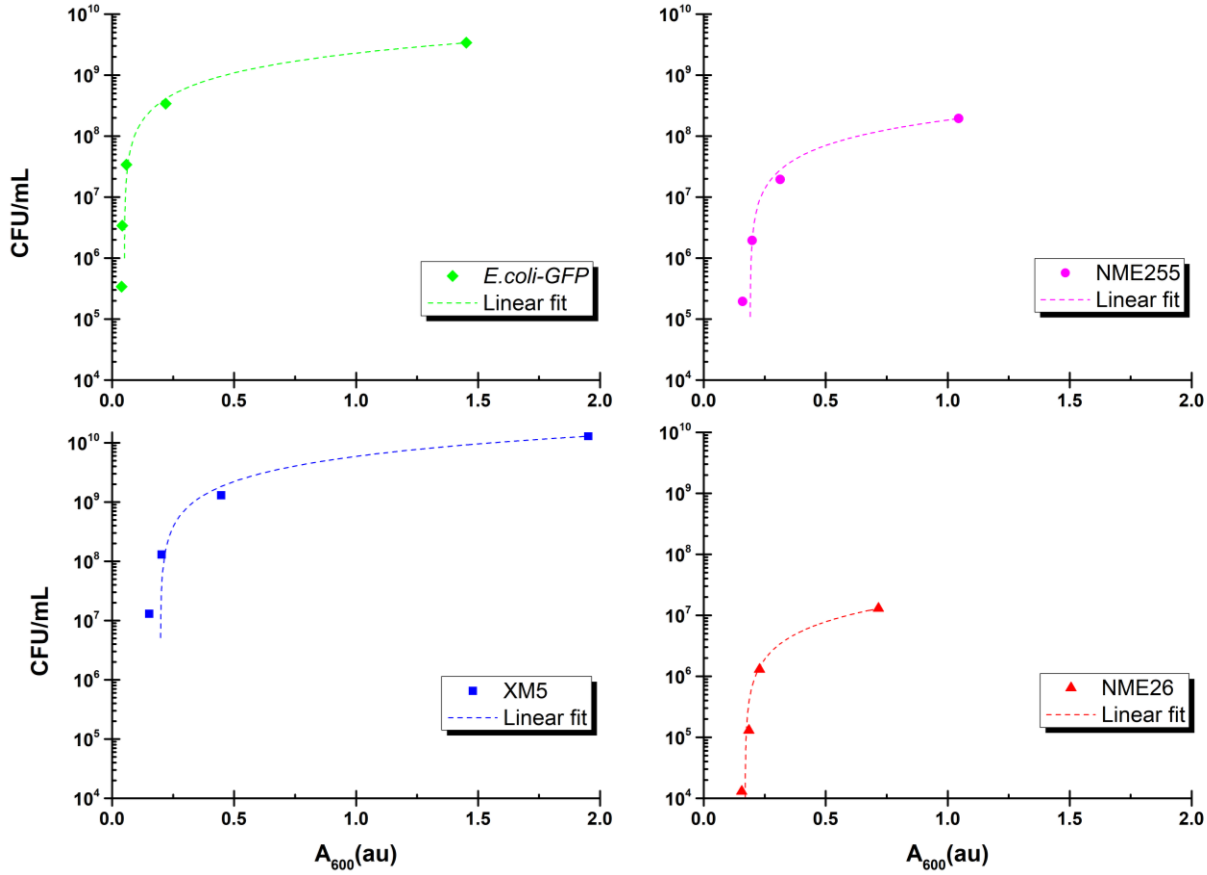

Figure S2. Fitted curve plots. Relation between the number of bacteria per milliliter (CFU mL^{-1}) and the optical density measured at 600 nm (A_{600}) for each of the bacterial strains used in this work.

Table S1. Parameters obtained by linear fit of the relation between CFU mL^{-1} vs A_{600} for each of the bacterial strains used in this work.

Equation	y = a + b*x			
	E. coli-GFP	NME255	XM5	NME26
Residual Sum of Squares	4.25E+17	6.37E+15	1.25E+14	1.89E+11
Pearson's r	0.998	0.999	0.998	0.999
Adj. R-Square	0.995	0.999	0.993	0.998
		Value	Standard Error	
E. coli-GFP	Intercept	-1.46E+09	3.15E+08	
	Slope	7.37E+09	3.12E+08	
NME255	Intercept	-1.21E+08	2.47E+07	
	Slope	2.42E+09	3.75E+07	
XM5	Intercept	-4.30E+07	6.14E+06	
	Slope	2.26E+08	1.10E+07	
NME26	Intercept	-4.02E+06	2.65E+05	
	Slope	2.37E+07	6.71E+05	

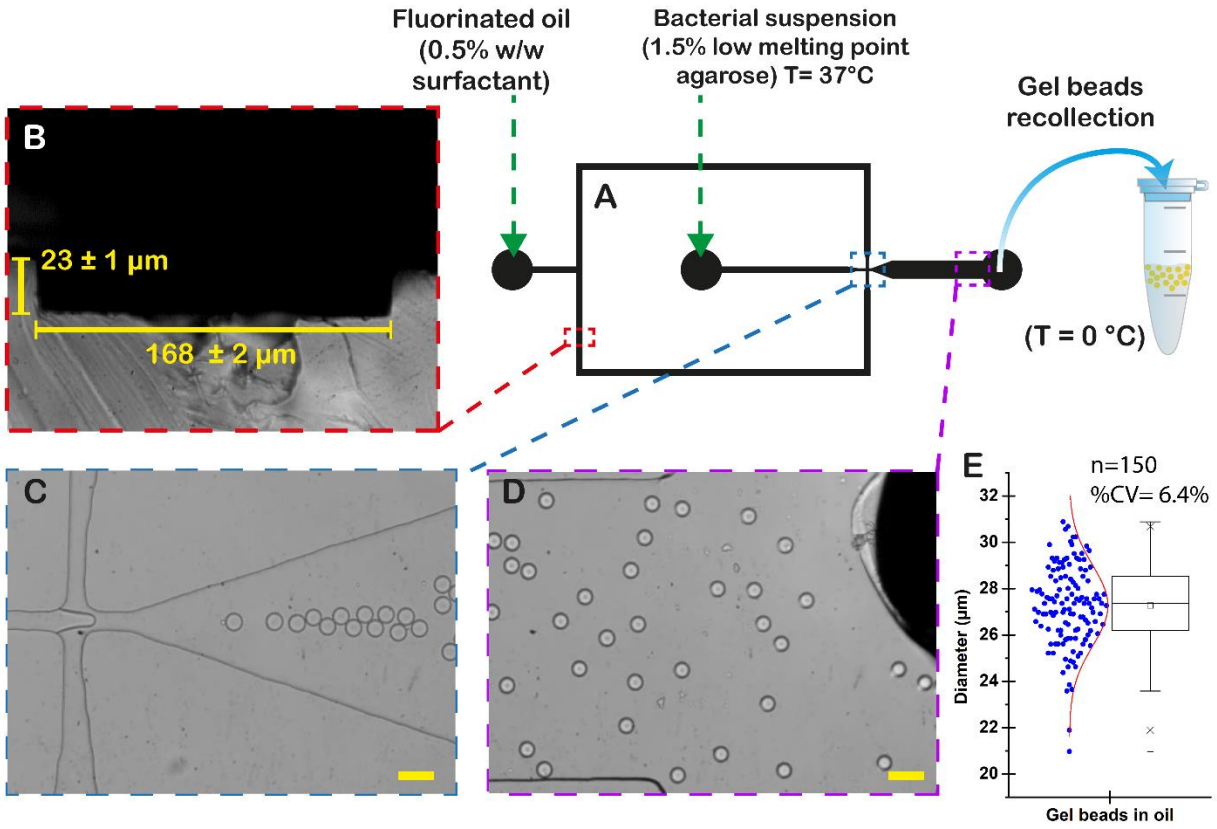

Figure S3. (A) Microfluidic channels design for gel beads formation. A flow-focusing design was used with two inlets: one for injecting fluorinated oil (HFE-7500) with 0.5 % w/w of the fluorosurfactant Bio-RAD; and the second for injecting bacterial suspensions. (B) Cross section of PDMS of a PDMS replica of the channel in which the fluorinated oil flows through. (C). Flow focusing junction of the flow of fluorinated oil with the flow of bacteria suspension. The immiscible phases are intercepted and the aqueous phase segregates in monodispersed water in oil droplets. Droplets are formed at frequencies of 700 Hz, scale bar 50 µm. (D) Droplets formed flow through the channel and are collected at the outlet with PTFE tubing, scale bar 50 µm. (E) Distribution of diameters obtained from a sample of gel beads, mean=27±2 µm.

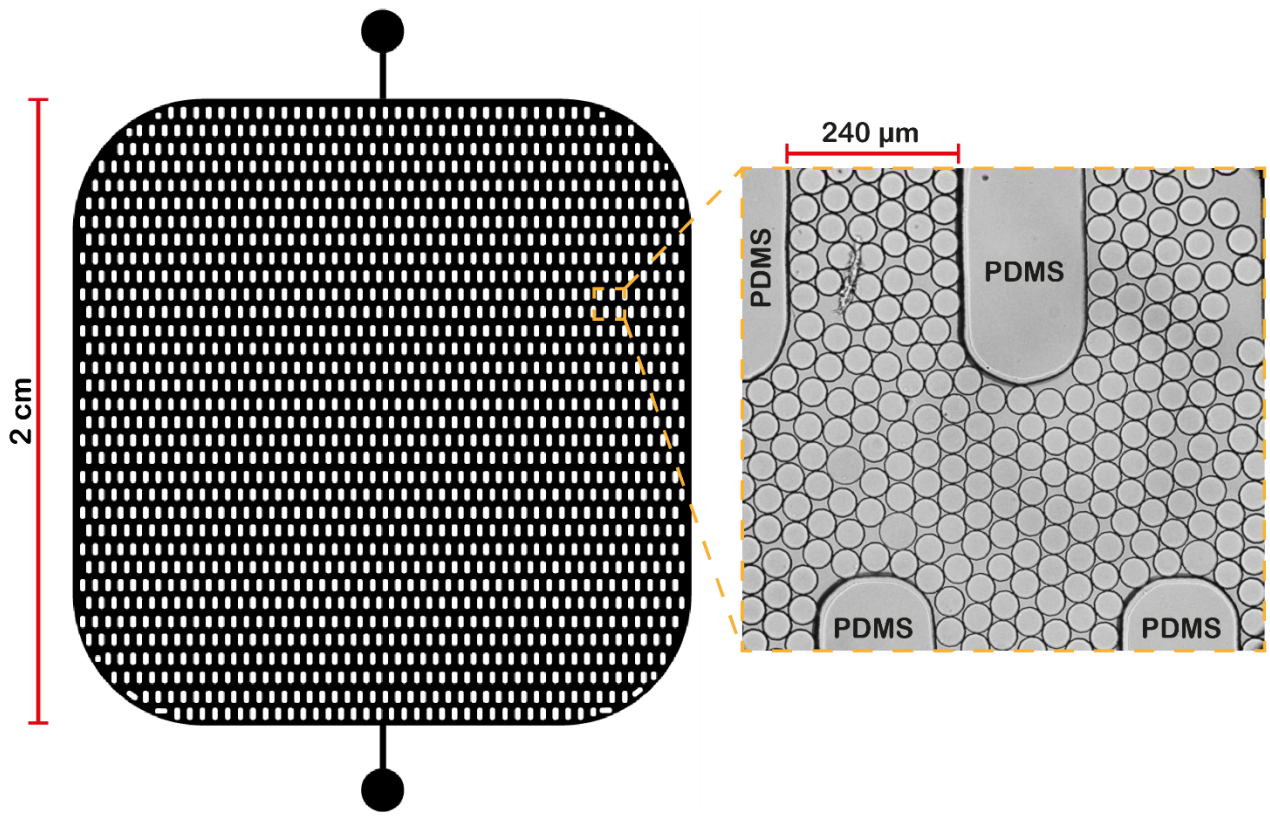

Figure S4. Gel beads observation chamber design.

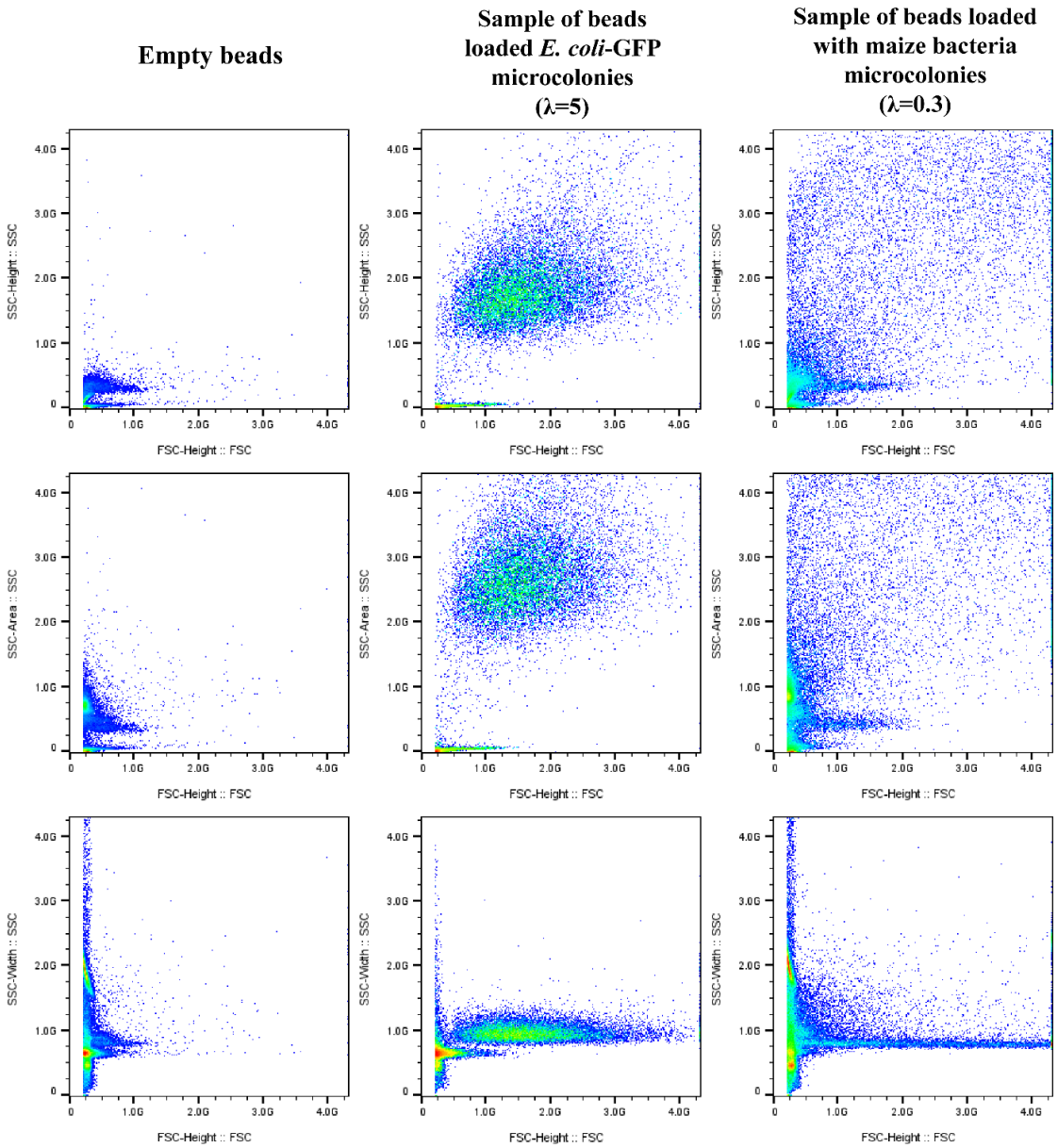

Figure S5 (Part A). Using FACS we performed an in-depth independent analysis of all the possible combinations of scatter signals (SSC vs FSC) obtained for three different gel beads samples: empty beads; beads loaded with *E. coli*-GFP microcolonies (λ=5); and beads loaded with microcolonies of one of the strains isolated from maize (λ=0.3). **Part A** of this figure shows all the possible combinations of FSC-Height with the three different SSC signals obtained for gel beads using FACS. **Part B** of this supplementary figure on the next page illustrates all the possible combinations of FSC-Area with SSC signals. Generally, FSC-Area produces signals that tail to the right more than FSC-Height. Specifically, when FSC-Area was used for bacteria-loaded beads, a more significant proportion of the registered hits saturated the detector and fell on the right limit of the X-axis. This prompted our decision to favor FSC-Height over FSC-Area. Regarding SSC signals, the SSC-Height signals for empty beads consistently remained at values lower than 0.75 units, while the populations of bacterial-loaded beads were differentiated at values higher than 0.75 units. In contrast, when SSC-Area or SSC-Width were used, the signals for empty beads registered with FACS were more widely distributed along the entire Y-axis range,

leading to an overlap between the population of empty beads and the population of gel beads filled with microcolonies of strains isolated from maize. In our experiments, SSC-Height versus FSC-Height represents the most suitable parameter association for discriminating between empty and bacterial-loaded beads.

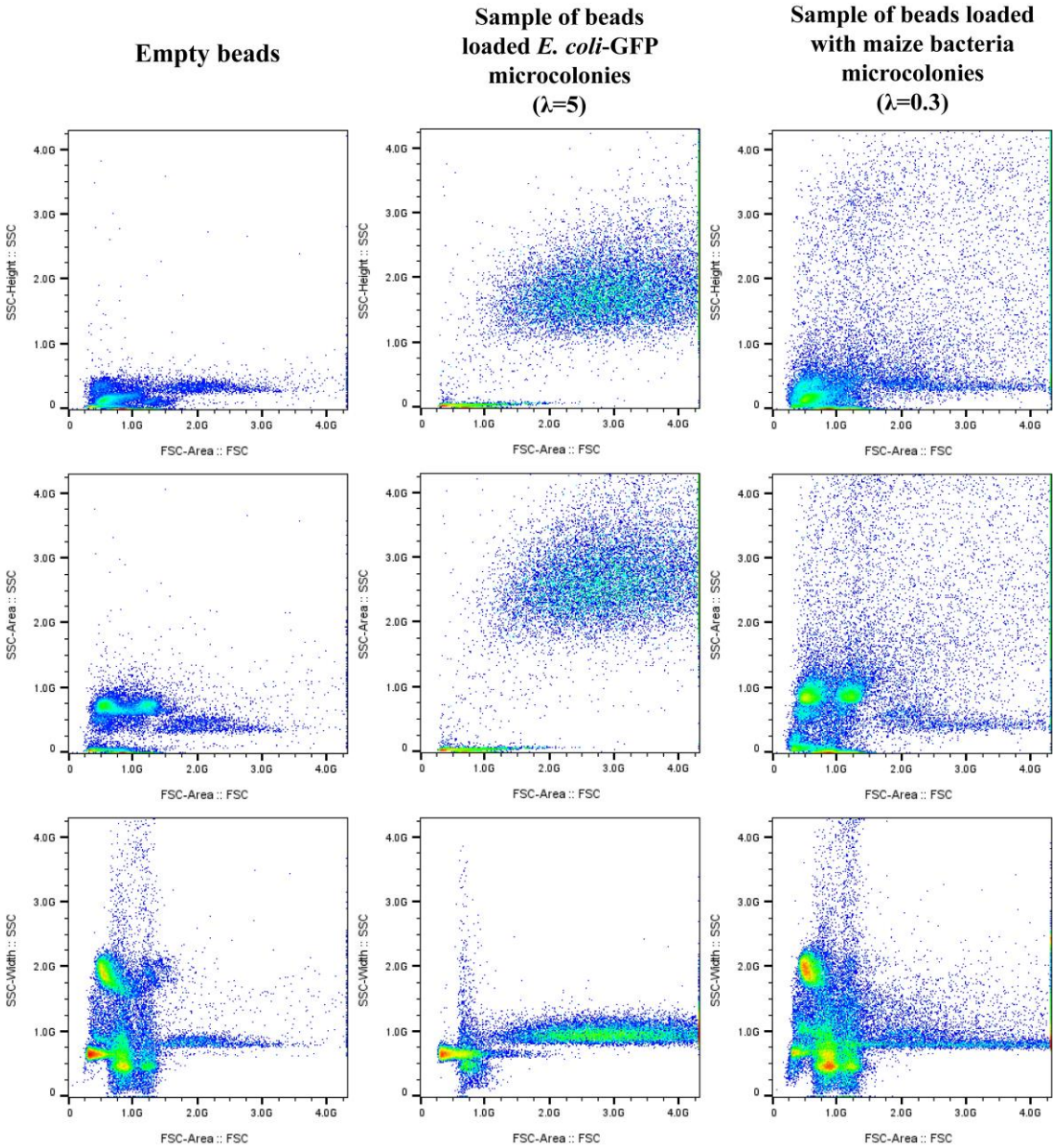

Figure S5 (Part B). All possible combinations of FSC-A versus SSC scatter signals obtaining using FACS for three different samples of gel beads: empty microgels; microgels loaded with E. coli-GFP microcolonies (λ=5); and microgels loaded with microcolonies of one of the strains isolated from maize (λ=0.3).

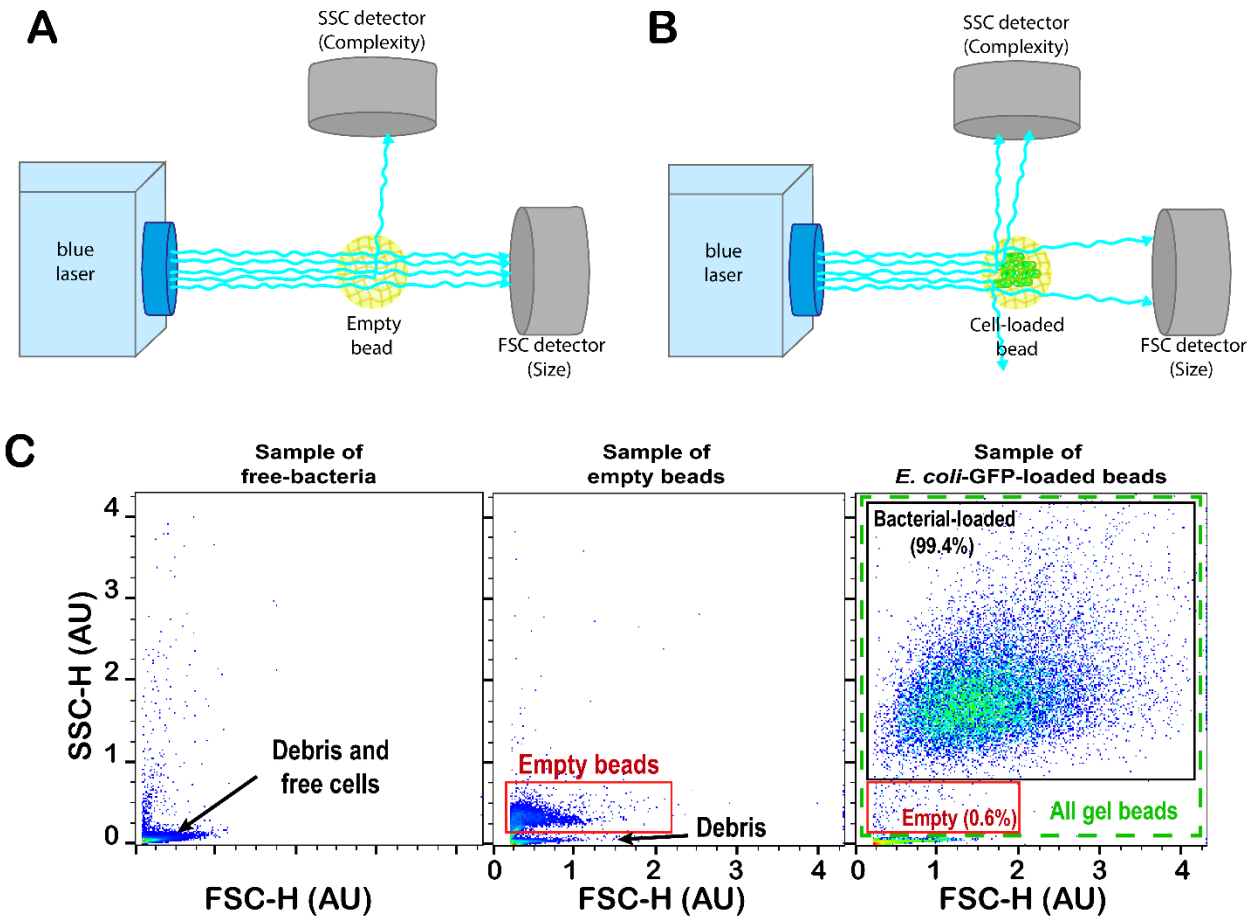

Figure S6. Schematic representation of side and forward light scattering when (A) empty beads or (B) bacterial-loaded gel beads are analyzed by flow cytometry. (C) Dot scatter plots obtained by FACS for a non-encapsulated bacteria suspended in liquid media 2YT; empty gel beads sample; and a sample of gel beads with *E. coli-GFP* microcolonies encapsulated. Based on the scatter signal obtained for free-bacteria, the scatter region of all gel beads was set into the green gate. Into this region, empty beads were enclosed into the red gate, and gel beads with *E. coli-GFP* microcolonies encapsulated were discriminated into the bacterial-loaded gate (black gate in the third panel). The percentage of empty beads present in the sample of beads with *E. coli*-GFP encapsulated agrees with theoretical Poisson calculations (0.7% of empty and 99.3% of bacteria-loaded beads).

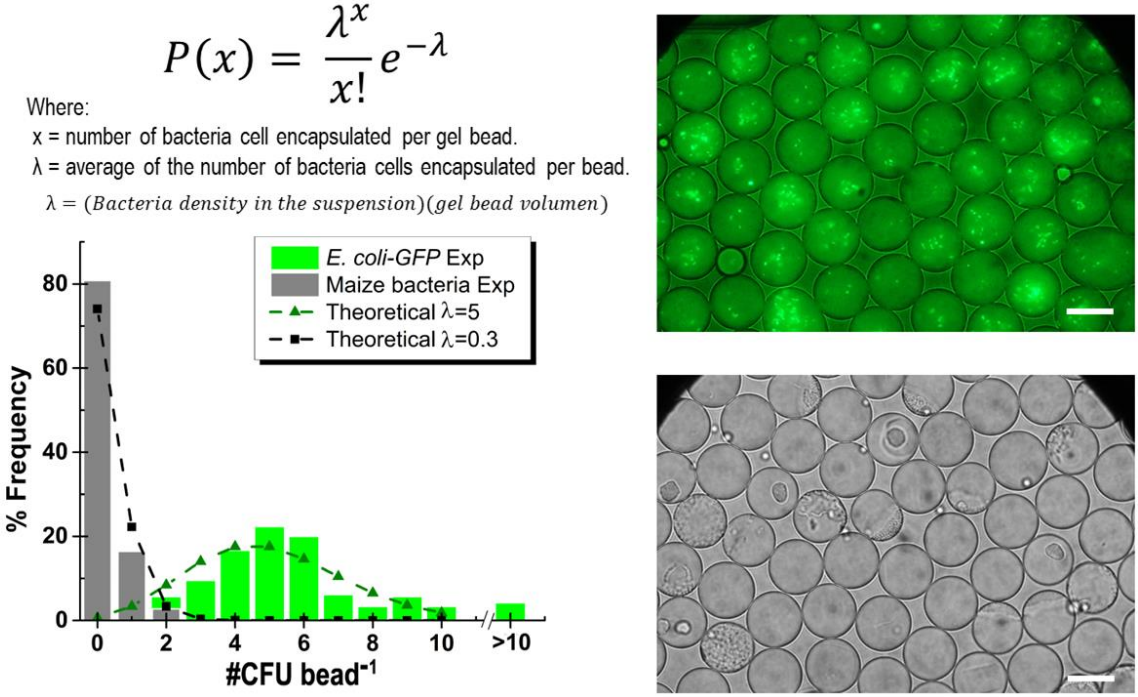

Figure S7. Top left, Poisson distribution equation. Bottom left, theoretical Poisson distribution (dotted lines) and experimental (bar graphs) number of cells per bead at the different average of bacteria per bead (λ) used in this work. Top right, typical fluorescence microscopy image of *E. coli-GFP* cells encapsulated into gel beads of 10 µL (λ = 5.0). Photos were taken just after gel bead formation. Bottom right, typical bright-field microscopy images of the mixture of the three maize bacteria isolated from maize encapsulated in gel beads (global λ = 0.3 for the mixture, each strain contributes with 0.1 units). Photos were taken after 48 h incubation at 27 °C of the gel bead samples.

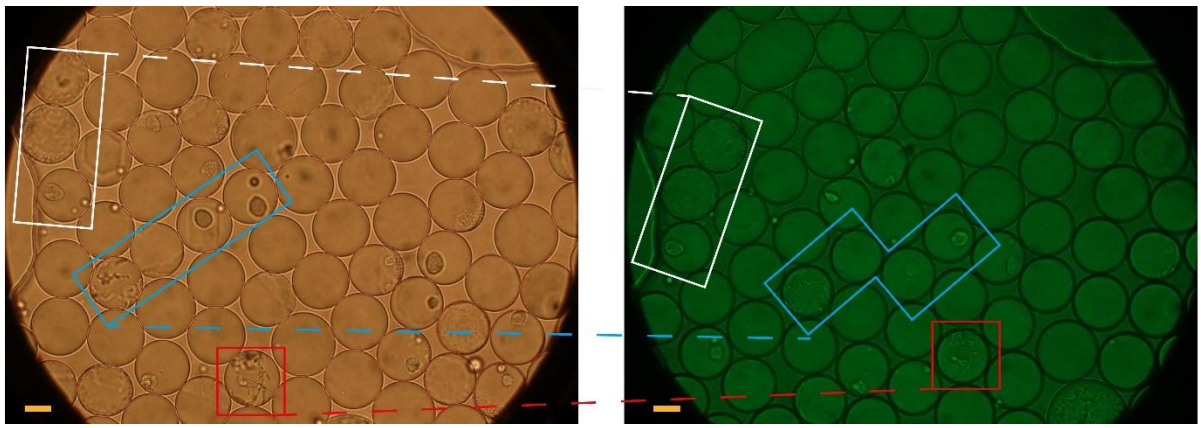

Figure S8. Representative microscopy images of a sample of gel beads encapsulating microcolonies from the three bacterial strains isolated from maize. On the left is the bright-field image. On the right is the fluorescence field image, which shows that the three bacterial strains are non-fluorescent. The bright-field image provides a clearer view of the growth details of the encapsulated microcolonies. Due to random movement within the observation chamber, the beads shifted their position from one photo to another. However, the white, blue, and red rectangles indicate examples of corresponding beads in the bright-field and fluorescence images. Scale bar 10 µm

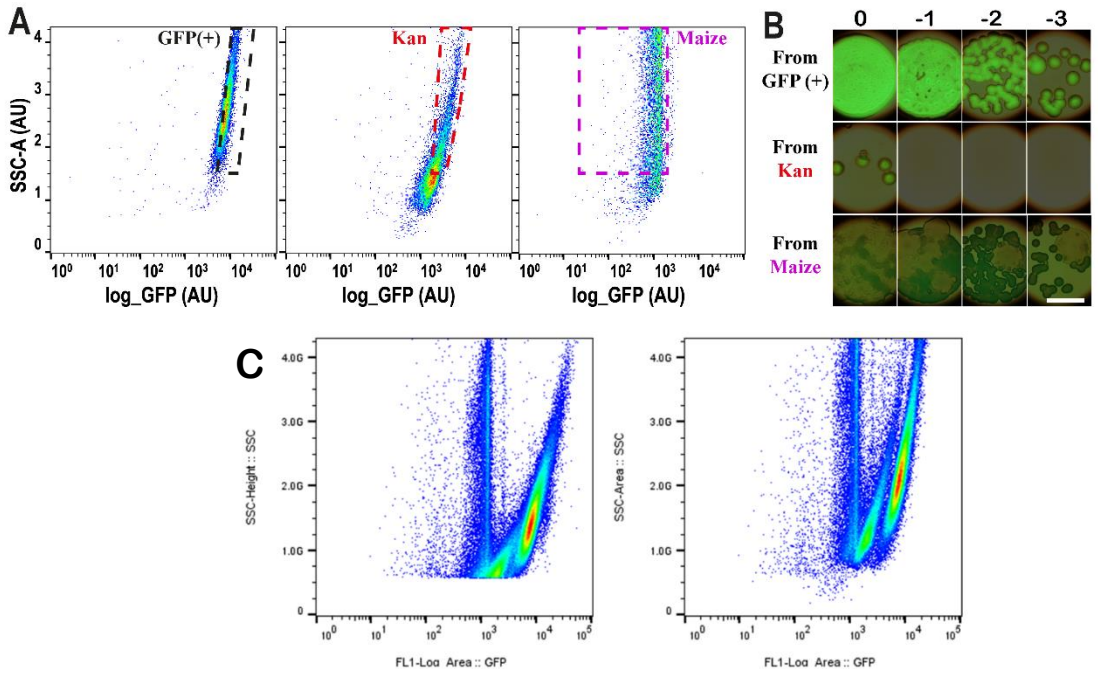

Figure S9. (A) SSC-A vs fluorescence intensity scatter plots obtained from incubated gel beads samples. From left to right: *E. coli*-GFP bacteria in gel beads without antibiotic; gel beads with *E. coli*-GFP and kanamycin (100 µg/mL); the three maize bacteria encapsulated within gel beads. (B) Bacteria colonies recovered on agar plates inoculated with the gel beads retrieved by FACS at gates GFP(+), Kan and maize (dashed boxes in SSC-A vs log_GFP scatter plots), scale bar 0.5 cm. (C) Flow cytometry signals were acquired from a mixture of control bead samples loaded with maize bacteria, *E. coli*-GFP with kanamycin, and E. coli-GFP without antibiotics in a 1:1:1 ratio. The scatter plot on the left displays SSC-H (side scatter) vs fluorescence intensity, while the scatter plot on the right represents SSC-A (side scatter) vs fluorescence intensity. Notably, the SSC-A vs fluorescence intensity combination enables superior discrimination between the different gel bead populations, providing clearer differentiation.

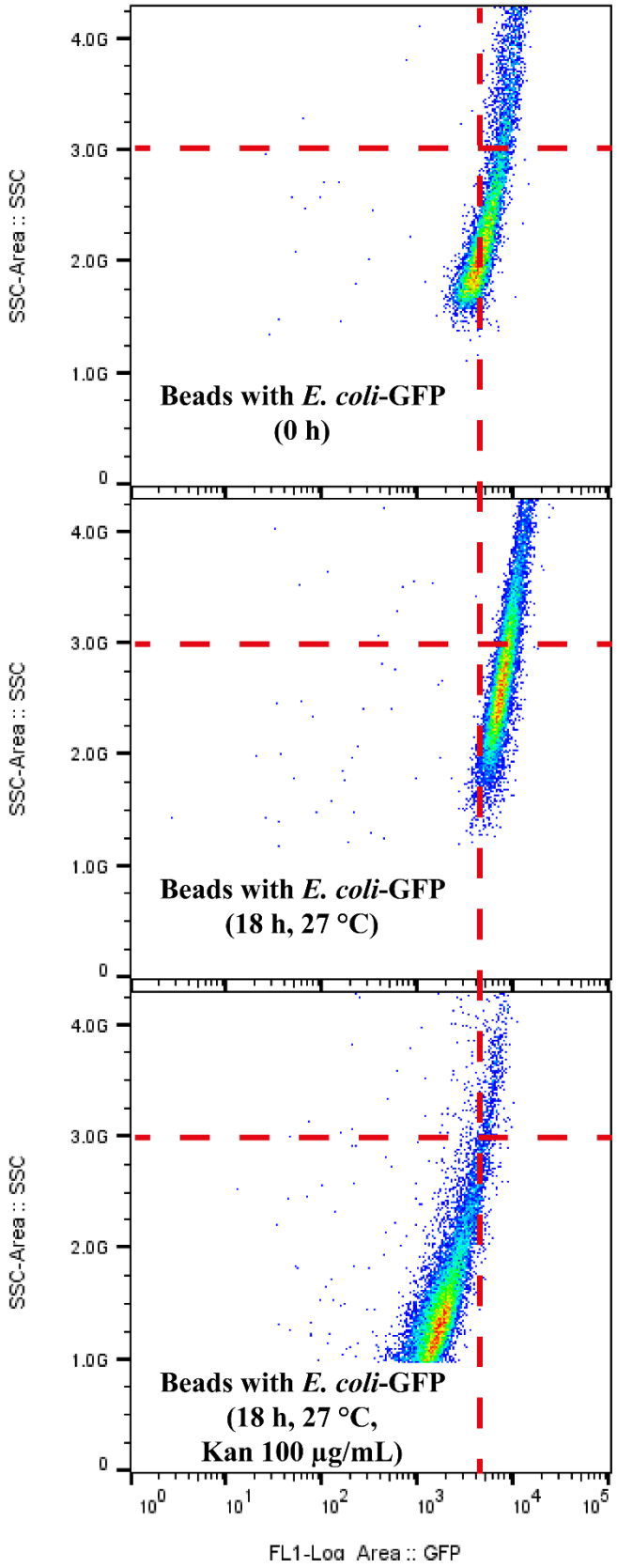

Figure S10. Comparison of SSC-A vs. fluorescence intensity plots obtained from gel beads loaded with *E. coli*-GFP and incubated under various conditions. When gel beads were loaded with *E. coli*-GFP (0 h) and left without antibiotics for 18 h, the entire bead population shifted towards higher fluorescence and slightly higher SSC-A values. In contrast, when gel beads were loaded with *E. coli*-GFP and kanamycin and incubated for 18 h, the signals shifted to lower SSC-A and fluorescent values. This indicated that the majority of *E. coli*-GFP cells disappeared from the beads. However, some gels with SSC-A values greater than 3.0G maintained their fluorescence intensity within the same range as the non-incubated beads loaded with *E. coli*-GFP. These observations suggest that in the gel beads that had a high initial density of encapsulated bacteria, the kanamycin concentration was insufficient to disintegrate all the bacteria. Instead, it solely prevented microcolony development. In contrast, the kanamycin concentration effectively achieved bacterial disintegration in gel beads with initially fewer encapsulated bacteria, resulting in lower fluorescence intensity than the sample incubated without antibiotics.

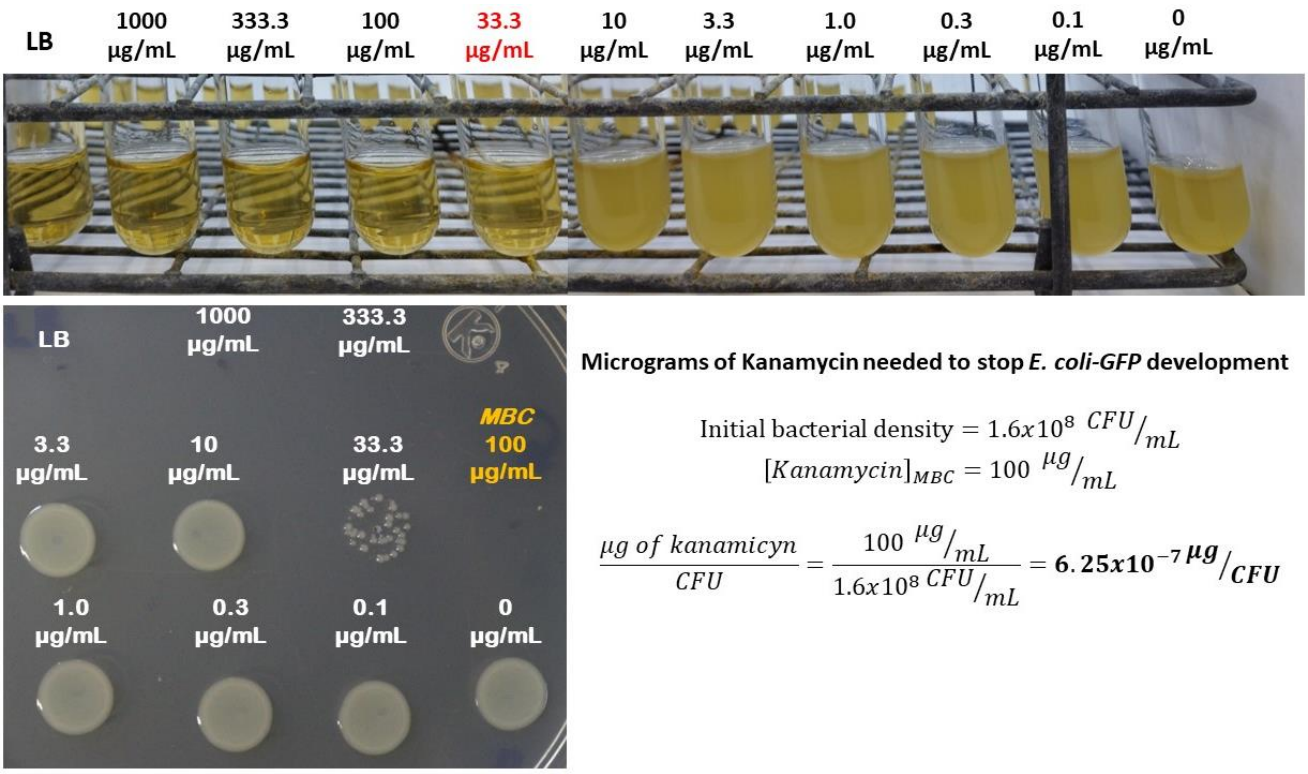

Figure S11. Minimal inhibitory activity (MIC) and Minimal Bactericidal activity (MBC) of Kanamycin against *E. coli-GFP*.

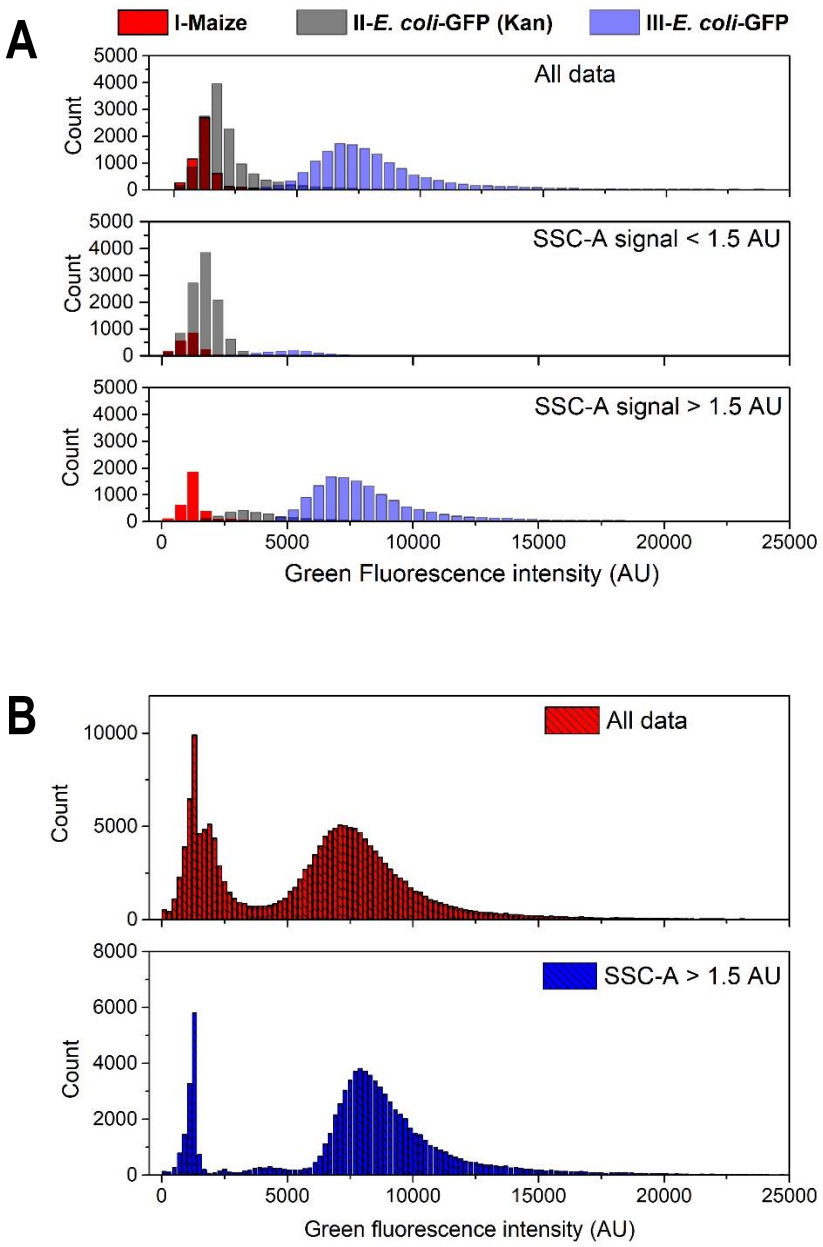

Figure S12. (A) Histograms of green fluorescence intensity were generated from FACS data independently for a sample of gel beads loaded with microcolonies of maize bacteria; *E. coli*-GFP treated with Kanamycin; or with *E. coli*-GFP microcolonies. Each histogram was generated using different SSC-A intensity thresholds. (B) A 1:1:1 mixture of the three independent samples was made and analyzed by FACS. Data was used to generate histograms using the same SSC-A thresholds as in (A).

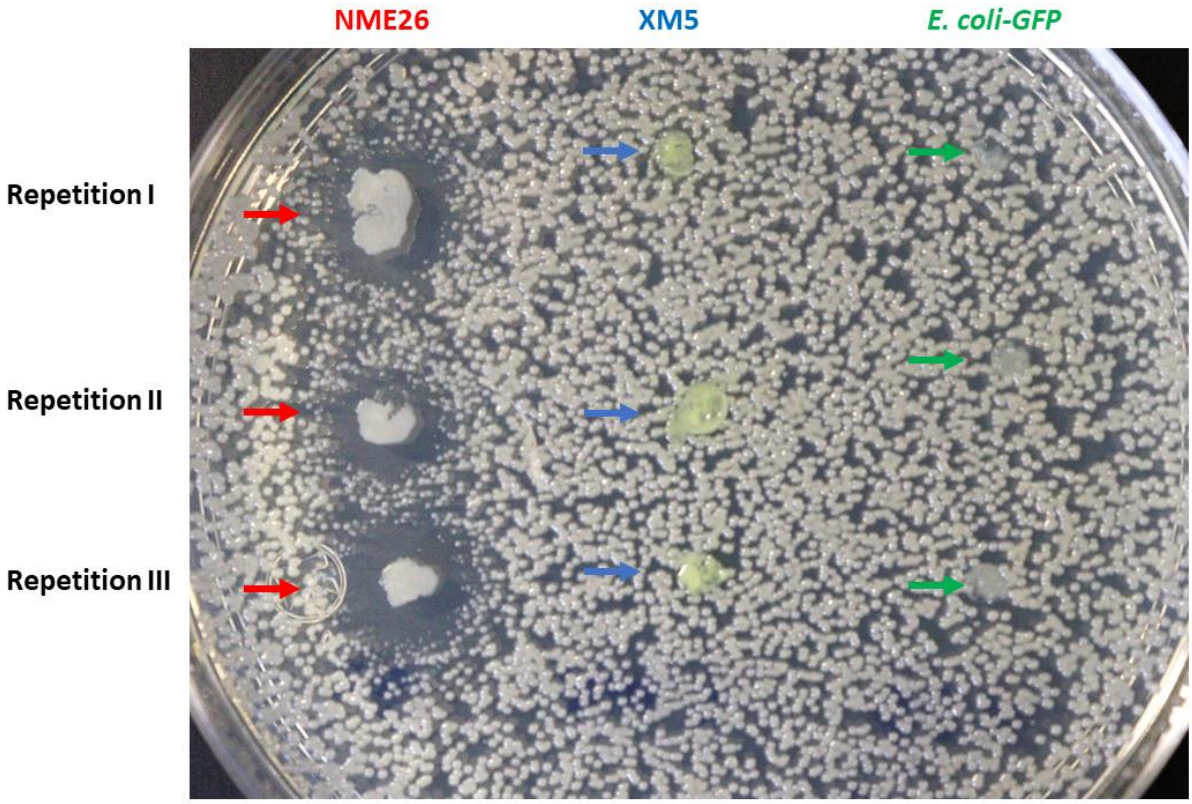

Figure S13. Agar plate assay to determine the antagonistic activity of NME26 (left), XM5 (middle) and *E. col-GFP* (right) against NME255 (on the agar surface). The entire agar surface was inoculated with NME255, and spots of the other strains were inoculated on the agar with a toothpick. After 48 h incubation at 27 °C, only NME26 develops inhibition halos indicating bactericidal activity against NME255.

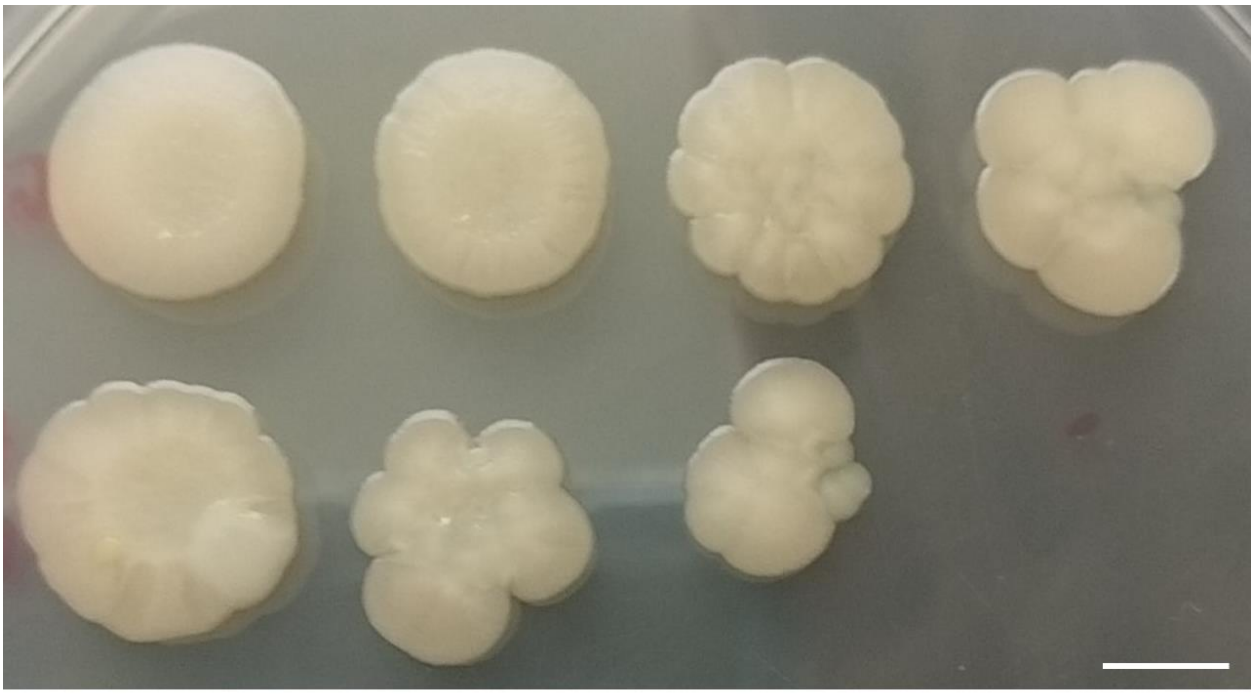

Figure S14. Colony development on agar plates inoculated with gel beads containing NME255. Photos were taken after 48 h of incubation at 27 °C. Scale bar 0.5 cm.

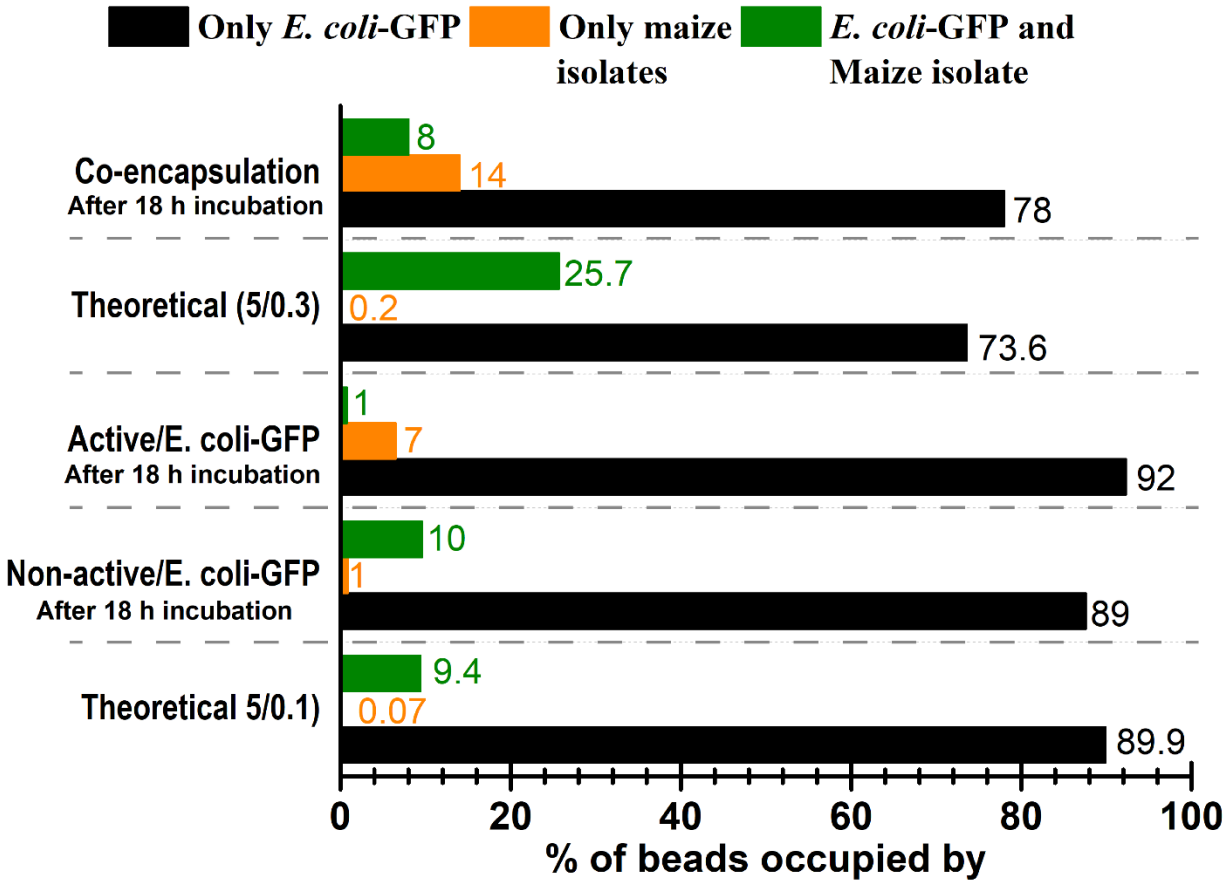

Figure S15. Theoretical and experimental Poisson distribution of bacteria co-encapsulated in gel beads, experimental data was evaluated using fluorescence and bright-field microscopy.

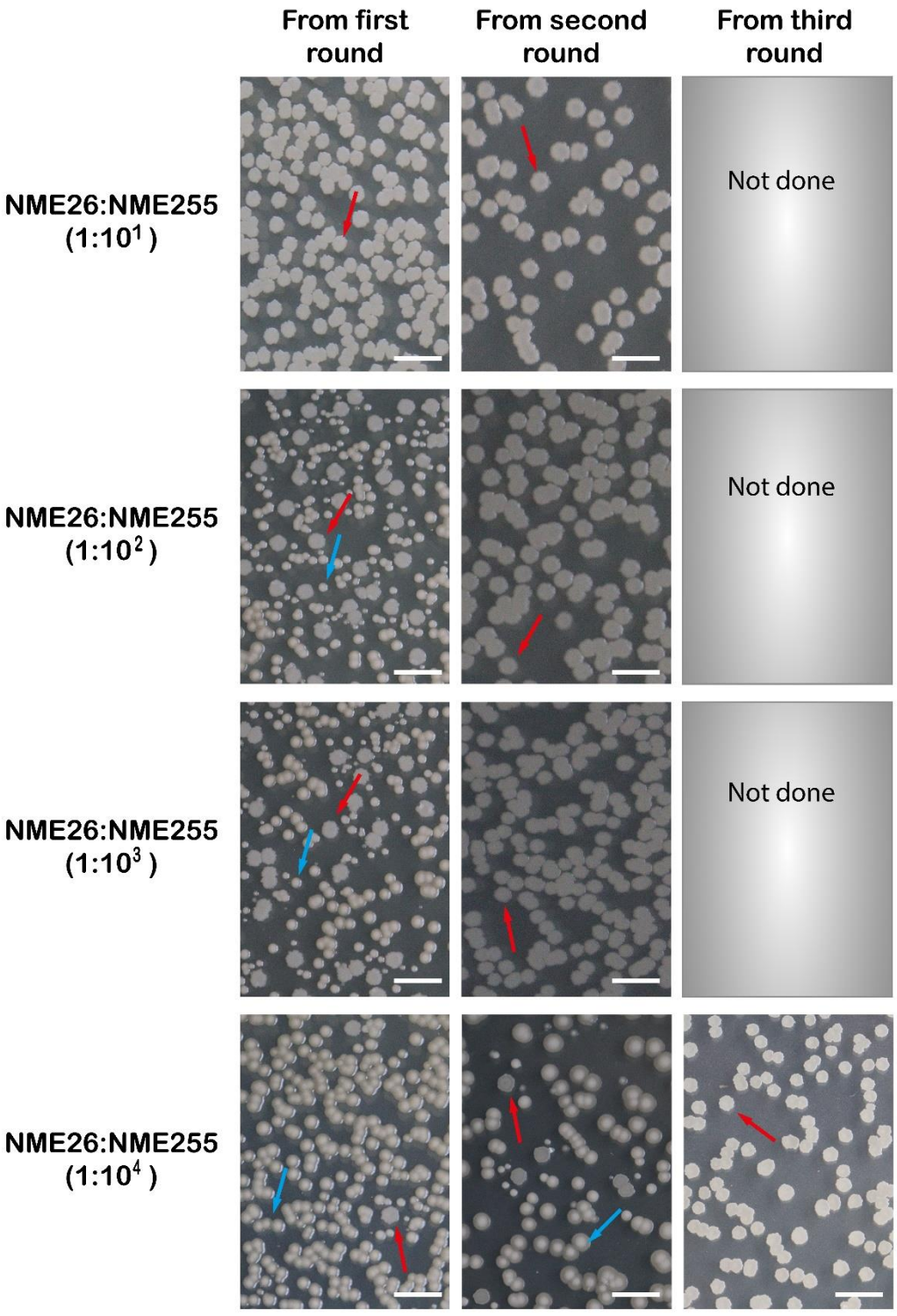

Figure S16. Representative images of agar plates inoculated with gel beads recovered from GFP (-) for dilution of NME26 with NME255 and after each round of co-encapsulation. Images were taken after 48 h of incubation at 27 °C. The arrows point to an example of some of the maize colonies present in the dish: red, NME26; blue NME255.

Table S2. Comparative table between our methodology and 6 relevant similar methodologies for the sorting and recovery of microfluidic particles loaded with cells or PCR products.

Reference*	Analyzed particle	Material loaded	Particle size (µm)	Technique used for sorting	Event rate for Sorting (events/s)	Single particle recovery efficiency (%)
This work	Gel beads	Cells	27±1	FACS	1 000	16
(36)	Gel beads	Cells	90-500	FACS	300	Not reported
(39)	Gel beads	Cells	120-200	FACS	1 000	Not reported
(43)	Gel beads	Cells	∼27	FACS	3 000	Not reported
(41)	Double emulsions w/o/w	Cells	∼25	FACS	30 000	Not reported
(29)	Double emulsions w/o/w	PCR products	27.6-48.4	FACS	300	∼70
(52)	Double emulsions w/o/w	PCR products	∼30	FACS	200-10 000	Not reported
(25)	Single emulsions w/o	Cells	70-80	FADS	10-50	Not reported

* Reference number corresponds to numeration in the main article.

During particle analysis with FACS, three fundamental parameters related to the technique's separation capacity can be established (*Brower 2020; Rodrigues 2016; Osborne 2010*). Firstly, the sorting throughput corresponds to the rate at which the equipment analyses all particles within a sample. This parameter primarily depends on the sample's particle density and the injection flow rate into the equipment. For the analysis of microfluidic particles housing microorganisms or PCR products, this parameter typically ranges between 200 and 30,000 events per second, but better target recovery is obtained at low event rates (*Lim 2013*). At the events rate we used, we obtained a target specificity recovery (percentage of recovered particles with the desired properties) higher than 95% (Movie S2).

The second key parameter is the sort rate, which represents how frequently the sorted particles are directed to their respective reservoirs based on the chosen gate strategy. This parameter can vary significantly between experiments, as it depends on the density of particles with the required properties to be sorted into each gate set during sample analysis. Typically, our sort rates fell

between 400 and 4 selected particles per second within the GFP (+) and GFP (-) gates, respectively (Table S3). Notably, methodologies for microfluidic particle sorting with FACS rarely report these specific data.

Table S3. Sorting efficiency attained after analyzing and sorting a representative sample of bacteria-loaded beads. We combined the three bacteria from maize with *E. coli*-GFP in the same suspension and co-encapsulated them into picoliter gel beads. We set $\lambda = 5$ for *E. coli*-GFP and $\lambda = 0.3$ for the mixture of maize bacteria. After 18 h of incubation, the sample was analyzed using FACS and sorted using the GFP (-) and GFP (+) gate strategy described in the main text.

	GFP (+)	GFP (-)
Sorting rate (events/s)	400	4
Σ Sort (events)	505 140	6 370
Σ Abort (events)	16 640	620
Efficiency (%)	97	90

- Event-rate= 1000 events/s Event count = 639 230

Lastly, the third parameter concerning FACS's particle selection capability is the sorting efficiency, denoting the actual number of recovered particles in a reservoir with a desired characteristic, in relation to the number of sorted particles recorded by the equipment with those properties. Previous studies on double emulsion sorting with FACS revealed a sorting efficiency of approximately 70% for a single particle (*Brower 2020*). In our case, the recovery efficiency for a single gel bead was 16% for a non-optimized process (Figure S17). However, sort efficiency can be enhanced by calibrating drop delay within the FACS equipment (*Brower 2020*). Additionally, employing FACS recovery in 96-well plates for gel beads loaded with *E. coli*-GFP microcolonies, we determined a 75% probability of recovering particles within the reservoirs when selecting fewer than ten particles per well, increasing to 100% for selections of more than 33 particles within the same reservoir (Figure S18). Given that our methodology consistently involved selecting more than 100 particles per reservoir, we can confidently assert that we recovered the targeted gel beads.

Figure S17. Gel beads loaded with *E. coli*-GFP microcolonies were analyzed and sorted with FACS. A single sorted bacteria-loaded bead was deposited on the lid of a 96-well plate covered with LB-Agar. In such a way, using FASC, the sorted gel beads were deposited directly on a culture plate with a solid medium. After 24 h of incubation at 27 °C, bacterial growth on agar was evaluated. Fifteen colonies were recovered from the 96 desired, giving a sort-efficiency of 15.6%.

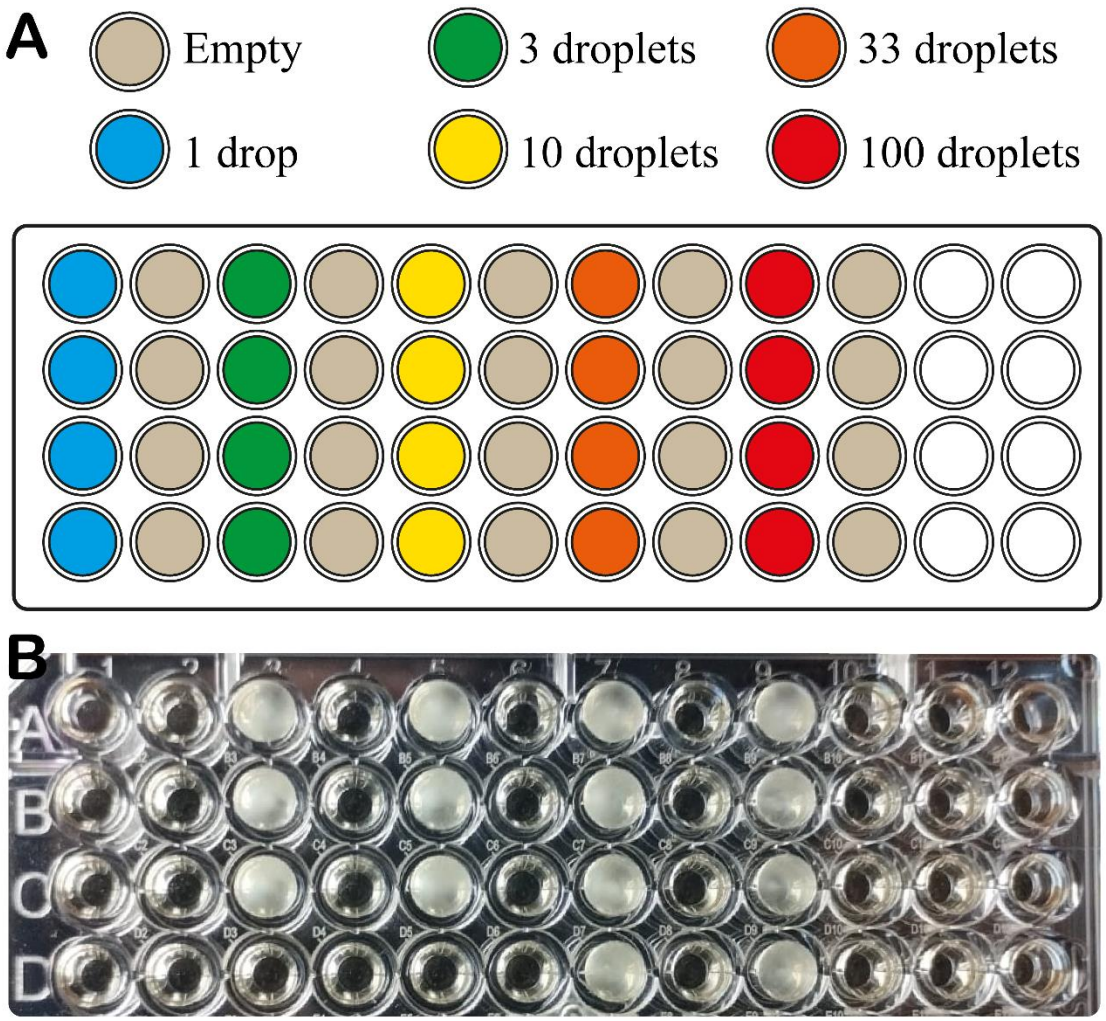

Figure S18. (A) Gel beads loaded with *E. coli*-GFP were analyzed and sorted with FACS. Different amounts of selected gels were deposited directly into wells filled with LB liquid media in a 96-well plate as indicated in the color image. (B) The 96-well plate with the recovered beads was incubated for 24 h at 27 °C and then bacterial growth was evaluated within each well.

Movie S1. Microfluidic channels design to gel beads formation. A flow-focusing design with two inlets was used. The first inlet was used for the injection of fluorinated oil (HFE-7500) with 0.5% w/w of the fluorosurfactant (RAN Biotechnologies). The second inlet was used for the injection of bacterial suspensions. Droplets were formed at frequencies of 700 Hz, collected at the outlet with a PTFE tubing and received into a microtube immersed in ice for gel beads induction.

Movie S2. Gel beads encapsulating *E. coli-GFP* fluorescent microcolonies were mixed with gel beads encapsulating non-fluorescent microcolonies of *E. coli-wt* in a proportion 1:4, respectively. The gel beads mixture was analyzed and sorted with FACS. Gel beads with fluorescent microcolonies encapsulated were sorted into GFP (+) gate and gel beads with non-fluorescent microcolonies were sorted into GFP (-) gate. Pre-sort and recovered gel beads were observed by bright-field and fluorescence microscopy.

References for Supplementary Information file

- Brower, K. K.; Carswell-Crumpton, C.; Klemm, S.; Cruz, B.; Kim, G.; Calhoun, S. G. K.; Nichols, L.; Fordyce, P. M. *Lab Chip* **2020**, *20* (12), 2062–2074.
- Lim, S. W.; Abate, A. R. *Lab Chip* **2013**, *13* (23), 4563–4572.
- Osborne, G. W. *Cytometry Part A* **2010**, *77* (10), 983–989.
- Rodrigues, O. R.; Monard, S. *Cytometry Part A* **2016**, *89* (6), 594–600.